



ELSEVIER

Physica A 235 (1997) 257–268

PHYSICA A

# Electric double layers around finite-size clay particles

Jean-Pierre Hansen\*, Emmanuel Trizac

*Laboratoire de Physique (U.R.A. 1325 du CNRS), Ecole Normale Supérieure de Lyon,  
69364 Lyon Cedex 07, France*

---

## Abstract

The electric double layer of co- and counterions around a finite, disc-shaped, uniformly charged clay platelet in a spherical or cylindrical Wigner–Seitz cell is studied within the linearized Poisson–Boltzmann theory. Explicit expressions are obtained for the density profiles, in the form of series in Legendre or Bessel functions. The quadrupole moment and the free energy of the charge distribution are calculated as functions of clay and salt concentrations. In cylindrical geometry, swelling is shown to be restricted under the action of electrostatic forces alone.

*PACS:* 82.70.Dd; 68.10.-m

*Keywords:* Electric double-layer; Clay colloid suspension; Density profile; Poisson–Boltzmann theory

---

*This paper is dedicated to Rudolf Klein on the occasion of his 60th birthday*

## 1. Introduction

Clay colloid suspensions are lamellar polyelectrolytes made up of mesoscopic, thin crystalline platelets carrying structural charges (polyions) and microscopic co- and counterions (microions) dispersed in water [1]. In the initial stages of swelling, the platelets are stacked parallel to each other, separated by layers of aqueous electrolyte solution. As long as the spacing of the platelets is small compared to their lateral dimension (typically several hundred Å), the platelets may be modelled by infinite, uniformly charged planes, and the electrostatic problem reduces to a one-dimensional one. In this simple geometry, the non-linear Poisson–Boltzmann (PB) equation may be solved analytically in some specific situations (Gouy–Chapman theory [2]) and a large literature exists on electrostatically swollen lamellar phases (for some recent work, see e.g. [3, 4], and references therein).

---

\* Corresponding author.

However, in more dilute suspensions, the lamellar order is lost when the spacing between the platelets exceeds their lateral dimension. The finite size of the particles can no longer be ignored and the problem becomes fully three-dimensional. A complete statistical mechanics description of a system of arbitrarily oriented platelets and of much smaller microions constitutes a formidable challenge because: (a) the lack of spherical symmetry renders the electrostatic problem very complicated; (b) the considerable difference in length scales associated with polyions and microions precludes a symmetrical treatment of the two components. The latter difficulty may be overcome in simulations combining molecular dynamics (or Monte Carlo) methods and density functional theory [5]. While such a hybrid approach has proved very fruitful for spherical polyions (like micellar or charge-stabilized colloids), its extension to lamellar polyions poses technical difficulties which are presently being investigated.

In this paper, we examine the simpler problem of a single, circular platelet confined with its counterions and added salt to a Wigner–Seitz (WS) cell. The approximate mean-field-like reduction of the initial  $N$ -platelet problem to a one-platelet problem is based on the introduction of the WS cell, of volume  $v$  equal to the volume per platelet  $V/N$  in the suspension, which models in a very crude way the local environment of any one clay particle (cage effect) [6]. The shape of the WS cell and the boundary conditions are dictated by physical considerations, and by the requirement of simplicity to allow analytic calculations to be pushed as far as possible. In the present paper, we consider the cases of spherical and cylindrical WS cells; a spherical cage corresponds, physically, to the limit of low platelet concentrations where the latter may rotate almost freely, while a cylindrical cage is better adapted to concentrated stacked configurations.

## 2. Model

The clay particle is modelled by an infinitely thin, rigid disc of radius  $r_0$  carrying  $Z$  elementary charges  $-e$  assumed to be uniformly distributed over the surface. The charge density will be denoted by  $q = -Ze/(\pi r_0^2)$ . This is a reasonable representation of the synthetic laponite clay particles [7] which have a typical diameter of 250 Å and a thickness of 10 Å. The positive counterions and negative coions are assumed to be monovalent point ions, and water is assumed to be a continuum of dielectric constant  $\epsilon$  (“primitive model”).

The disc is placed at the centre of a Wigner–Seitz cell; the macroscopic concentration  $n = N/V$  of clay particles determines the volume  $v = 1/n$  of the cell. For a spherical cage of radius  $R$ , the radius is then univocally determined. For a cylindrical cell of radius  $R$  and height  $2h$ , only the product  $2\pi R^2 h = v$  is fixed. The aspect ratio  $R/h$  is determined by minimizing a free energy as discussed later.

For a suspension with a given global salt concentration  $n_s$ , calculations are carried out in the canonical ensemble, where the numbers  $N_+$  and  $N_- = N_+ - Z$  of counterions and coions in the WS cell are fixed by  $N_- = v n_s$  and the charge neutrality constraint. For a suspension in osmotic equilibrium with a salt reservoir which fixes the chemical

potentials of the co- and counterions, the WS sample must be considered as an open system belonging to a grand canonical ensemble; the numbers of microscopic ions are determined by the condition that their chemical potentials match those in the salt reservoir.

Due to the lack of spherical symmetry of the polyion, the question of the adequate boundary conditions (b.c.) to be imposed at the surface of the WS cell is a delicate one. In the simpler case of a spherical polyion in a WS sphere, the symmetry naturally imposes that the electric field vanish at the surface of the sphere, on the assumption that the mean distribution of neighbouring polyions is essentially isotropic. In the case of a cylindrical WS cell, the symmetry of which is compatible with a circular polyion, we impose that the normal component of the electric field vanish everywhere on the surface of the cylinder, as periodicity and symmetry would require in a crystal-like configuration. However, for a WS sphere the symmetries of the cell and the polyion do not match, and the choice of b.c. is somewhat more arbitrary. In most subsequent calculations, quadrupolar b.c. will be imposed, i.e. the electrostatic potential at the surface of the sphere is required to coincide with the potential due to a point quadrupole fixed at the centre of the sphere; its value is required to match that calculated from the complete charge distribution (disc plus co- and counterions) inside the WS cell (self-consistency constraint). To test the sensitivity of the results to the choice of b.c., some results will be quoted, based on the condition that the normal electric field vanish on the surface of the sphere.

### 3. Solutions of the linearized Poisson–Boltzmann equation

Let  $\rho^+(\mathbf{r})$  and  $\rho^-(\mathbf{r})$  denote the local densities of counterions and coions, and let  $\rho_d(\mathbf{r})$  be the charge distribution on the surface of the polyion disc. The latter being assumed to be uniform,  $\rho_d(\mathbf{r})$  reads:

$$\rho_d(\mathbf{r}) = \rho_d(r, \theta) = \frac{q}{r} \delta(\cos \theta) \Theta(r_0 - r) \quad (\text{spherical coordinates}), \tag{1a}$$

$$\rho_d(\mathbf{r}) = \rho_d(r, z) = q\delta(z)\Theta(r_0 - r) \quad (\text{cylindrical coordinates}), \tag{1b}$$

where  $\delta$  and  $\Theta$  are the Dirac and Heaviside distributions, respectively. The PB theory results from the combination of the exact Poisson equation relating the electrostatic potential  $\varphi(\mathbf{r})$  to the local charge density:

$$\nabla^2 \varphi(\mathbf{r}) = -\frac{4\pi}{\epsilon} \rho_d(\mathbf{r}) - \frac{4\pi e}{\epsilon} [\rho^+(\mathbf{r}) - \rho^-(\mathbf{r})], \tag{2}$$

with the mean-field assumption

$$\rho^\pm(\mathbf{r}) = \rho_0^\pm \exp\{\mp \beta e \varphi(\mathbf{r})\}, \tag{3}$$

where  $\beta = 1/k_B T$  is the inverse temperature.

While in the limit of infinite dilution of polyions, where the WS cell occupies all space, the potential is conventionally assumed to vanish at infinity; this is no longer true

for finite concentration where the microions are confined. The potential is determined only within an additive constant, which will of course affect the prefactors  $\rho_0^\pm$  in Eq. (3). For a closed system (fixed salinity) the latter are determined by the normalization conditions

$$\rho_0^\pm \frac{1}{v} \int \exp\{\mp\beta e\varphi(\mathbf{r})\} d^3r = n_\pm, \quad (4)$$

where  $n_\pm$  are the overall concentrations of monovalent counterions and coions, which are related to the overall concentration of polyions by the electroneutrality constraint

$$n_+ - n_- = nZ. \quad (5)$$

With appropriate boundary conditions on the WS surface, the set of equations (2)–(4) may, in principle, be solved numerically. Such solutions have been obtained for the simple case of infinite polyion dilution (i.e. with the WS surface pushed to infinity) [8]. The numerical problem is more delicate to solve in a finite WS cell, and in this paper we seek an analytic solution of the *linearized* version of the PB equation; this is similar in spirit to the familiar Debye–Hückel theory of common electrolytes. It is convenient to express Eq. (3) in a slightly different form:

$$\rho^\pm(\mathbf{r}) = \rho_0^\pm \exp\{\mp\beta e[\varphi(\mathbf{r}) - \bar{\varphi}]\}, \quad (6)$$

where  $\bar{\varphi}$  is the mean potential in the WS cell:

$$\bar{\varphi} = \frac{1}{v} \int \varphi(\mathbf{r}) d^3r, \quad (7)$$

and the prefactors  $\rho_0^\pm$  are now in general different from those appearing in Eq. (3). In the perspective of linearization, it is reasonable to assume that  $\varphi - \bar{\varphi}$  yields on an average a smaller exponent than  $\varphi(\mathbf{r})$ . The linearized PB equation now reads:

$$\nabla^2 \varphi(\mathbf{r}) = -\frac{4\pi}{\epsilon} \rho_d(\mathbf{r}) - \kappa_D^2 \gamma_0 + \kappa_D^2 \varphi(\mathbf{r}), \quad (8)$$

where  $\kappa_D^2 = 4\pi\beta e^2(\rho_0^+ + \rho_0^-)/\epsilon = 1/\lambda_D^2$  is the squared inverse Debye length, and  $\gamma_0 = 4\pi e(\rho_0^+ - \rho_0^-)/(\epsilon\kappa_D^2) + \bar{\varphi}$ . Under these circumstances, the linearized version of the normalization condition (4) implies  $\rho_0^\pm = n_\pm$ .

### 3.1. Spherical coordinates

If the WS cell is a sphere of radius  $R$ , it is natural to adopt spherical coordinates with the polar axis orthogonal to the disc. Due to azimuthal symmetry,  $\varphi(\mathbf{r}) = \varphi(r, \theta)$ , and a solution of Eq. (8) is sought in the form of an expansion in Legendre polynomials:

$$\varphi(r, \theta) = \sum_{l=0}^{\infty} \varphi_l(r) P_l(\cos \theta), \quad (9)$$

where the sum is restricted to even values of  $l$  due to the symmetry  $\mathbf{r} \rightarrow -\mathbf{r}$ . The functions  $\varphi_l(r)$  are solutions of the radial differential equations. Due to the discontinuity of the electric field on crossing the uniformly charged disc, separate solutions of these equations must be considered for  $r \leq r_0$  and  $r > r_0$ , and the two solutions must be matched at  $r = r_0$ . In reduced units, the solutions  $\phi_l(x) = \beta e \varphi_l(\kappa_D r)$  may be combined in the form

$$\begin{aligned} \phi_l(x) &= \Theta(x_0 - x)\phi_l^<(x) + \Theta(x - x_0)\phi_l^>(x), \\ \phi_l^<(x) &= \beta e \gamma_0 \delta_{l,0} + a_l^< f_l(x) + b_l^< f_{-l}(x) + \zeta_l^* s_l(x), \\ \phi_l^>(x) &= \beta e \gamma_0 \delta_{l,0} + a_l^> f_l(x) + b_l^> f_{-l}(x), \end{aligned} \tag{10}$$

where  $x_0 = \kappa_D r_0$ , the functions  $f_{\pm l}(x) = \sqrt{\pi/(2x)} I_{\pm(l+1/2)}(x)$  are the modified spherical Bessel functions of the first and second kind,  $\zeta_l^* = (2l+1)P_l(0)/(\kappa_D b)$ ,  $b = e/(2\pi\ell_B q)$  is the Gouy length ( $b < 0$ ),  $\ell_B = \beta e^2/\epsilon$  is the Bjerrum length and the functions  $s_l(x)$  are defined by

$$s_l(x) = \sum_{\substack{n=0 \\ n \text{ even}}}^l \frac{\alpha_n^{(l)}}{x^{n+1}}, \quad \alpha_0^{(l)} = 1, \quad \alpha_{n+2}^{(l)} = \alpha_n^{(l)}[n(n+1) - l(l+1)]. \tag{11}$$

The coefficients  $a_l^<, b_l^<, a_l^>, b_l^>$ , are determined by matching the functions  $(\phi_l^<, \phi_l^>)$  and their derivatives at  $x = x_0$ , and by the boundary conditions at  $X = \kappa_D R$ . Two different boundary conditions have been considered. In the first, the normal component of the electric field at the surface is set to zero, i.e.  $\partial\varphi(r, \cos\theta)/\partial r|_{r=R} = 0$ . The potential is defined within the arbitrary constant  $\bar{\varphi}$  which may be taken equal to zero. In the second, the potential is required to reduce, for  $r=R$ , to the potential of a point quadrupole moment situated at the centre of the sphere, i.e.  $\varphi_Q(R, \cos\theta) = Q P_2(\cos\theta)/(\epsilon R^3)$ . The value  $Q$  of the quadrupole is matched self-consistently to that of the charge distribution inside the sphere (disc plus microions):

$$Q = Q_d + Q_\rho = \frac{2R^2}{5} \left[ 2R\varphi_2^>(R) - R^2 \frac{d\varphi_2^>(R)}{dR} \right]. \tag{12}$$

The coefficients  $(a_0^<, a_0^>)$  depend parametrically on  $\bar{\varphi}$ , whose value is univocally determined by the second self-consistency constraint:  $(\overline{\varphi} - \bar{\varphi}) = 0$ . The condition that the potential  $\varphi$  remain finite at the origin determines the coefficients  $b_l^<$ .

### 3.2. Cylindrical coordinates

For a cylindrical WS cell, one naturally uses cylindrical coordinates. The potential now depends on the coordinates  $(r, z)$ , and is expanded in a Bessel–Dini series [9] which is well adapted to the boundary conditions given below:

$$\varphi(r, z) = \sum_{n=1}^{\infty} A_n(z) J_0 \left( y_n \frac{r}{R} \right), \tag{13}$$

where  $y_n$  is the  $n$ th root of  $J_1(y) = -dJ_0(y)/dy = 0$ ,  $J_0$  and  $J_1$  are the Bessel functions of 0th and 1st order, and  $R$  is the radius of the cylinder. If  $2h$  is its height, the boundary conditions which we have imposed are

$$\left. \frac{\partial \varphi(r, z)}{\partial r} \right|_{r=R} = 0, \quad (14a)$$

$$\left. \frac{\partial \varphi(r, z)}{\partial z} \right|_{z=\pm h} = 0. \quad (14b)$$

With these conditions, one may assume that  $\bar{\varphi} = 0$ , without loss of generality ( $\varphi - \bar{\varphi}$  is independent of  $\bar{\varphi}$ ).

The differential equation for  $A_n(z)$  is easily solved leading to the final result

$$\begin{aligned} \phi(r, z) \equiv \beta e \varphi(r, z) = \beta e \gamma_0 + \frac{1}{\kappa_D b} \left( \frac{r_0}{R} \right)^2 \frac{\cosh[\kappa_D(h - |z|)]}{\sinh(\kappa_D h)} \\ + \frac{2 r_0}{b R} \sum_{n=2}^{\infty} \frac{A_n J_1(k_n r_0)}{y_n \sinh(h/A_n) J_0^2(y_n)} \cosh\left(\frac{h - |z|}{A_n}\right) J_0(k_n r), \end{aligned} \quad (15)$$

where  $A_n = R/\sqrt{y_n^2 + \kappa_D^2 R^2}$  and  $k_n = y_n/R$ . The resulting density profiles

$$\rho^{\pm}(\mathbf{r}) = n_{\pm} \{1 \mp \beta e [\varphi(r, z) - \bar{\varphi}]\} \quad (16)$$

are sensitive to the aspect ratio  $h/R$  for a given cell volume  $2\pi R^2 h$ . The ‘‘optimum’’ aspect ratio is determined by minimizing the free energy (which will be written down in the next section) with respect to this ratio.

In the limit  $r_0 = R \rightarrow \infty$ , the disc goes over to an infinite, uniformly charged plane in a WS slab of width  $2h$ , and the problem becomes one-dimensional: the potential depends only on  $z$  and the solution (15) reduces to

$$\phi(z) \equiv \beta e \varphi(z) = \beta e \gamma_0 + \frac{\cosh[\kappa_D(h - |z|)]}{(b \kappa_D) \sinh(\kappa_D h)}, \quad (17)$$

which is precisely the solution of the linearized Gouy–Chapman problem.

In the infinite dilution limit, the series in Eq. (15) goes over to an integral, and

$$\phi(r, z) = \frac{r_0}{b} \int_0^{\infty} dk J_0(kr) J_1(kr_0) \frac{e^{-\sqrt{\kappa_D^2 + k^2}|z|}}{\sqrt{\kappa_D^2 + k^2}}. \quad (18)$$

This expression yields

$$\phi(r = 0, z) = \frac{1}{\kappa_D b} \left[ e^{-\kappa_D |z|} - e^{-\kappa_D \sqrt{r_0^2 + z^2}} \right], \quad (19)$$

which reduces to the familiar exponential solution of linearized Gouy–Chapman theory in the limit  $r_0 \rightarrow \infty$ .

The reduced potential at the origin, as calculated from Eq. (19), is  $\phi(0) = \{1 - \exp(-\kappa_D r_0)\} / (\kappa_D b)$ . The same result is found in the spherical geometry, again in the infinite dilution limit (with the potential vanishing at infinity). From this result it is clear that linearization is justified provided  $|b| \gg \lambda_D$  (sufficient condition), i.e. in the limit of high salt concentration or low surface charge. A similar criterion is expected to apply for finite cells. Another sufficient, but rather academic, condition is that  $r_0 \ll \lambda_D$  and  $r_0 \ll |b|$ .

#### 4. Results

The density profiles  $\rho^\pm(\mathbf{r})$  are highly anisotropic, particularly so in the near vicinity of the disc. For that reason, a large number of terms are required in both expansions (9) and (15) to ensure adequate convergence, especially in the plane of the disc ( $\theta = \frac{1}{2}\pi$  or  $z = 0$ ). Examples of the resulting charge density  $\rho_c(\mathbf{r}) = \rho^+(\mathbf{r}) - \rho^-(\mathbf{r})$  are shown in Fig. 1 for a spherical WS cell. All figures correspond to  $Z = 100$  elementary negative charges on the disc,  $\epsilon_{CGS} = 78$  (water), and  $T = 300$  K.

An important characteristic of the electric double layer around the disc is the quadrupole moment (i.e. the  $zz$  component of the traceless quadrupolar tensor calculated in Cartesian coordinates with the  $z$ -axis orthogonal to the disc).  $Q$  may be calculated from Eq. (12) and is expected to depend on the polyion concentration  $n$  (or equivalently on the volume of the WS cell), on the salt concentration  $n_s$ , and on the geometry of the cell (sphere or cylinder). In the low-concentration limit  $n \rightarrow 0$ , the quadrupole moment must vanish, independently of the salt concentration [10]. Representative results are shown in Fig. 2. After a rapid initial variation at low  $n$ ,  $Q$  is seen to vary more slowly at high polyion concentration; in that region,  $Q$  is relatively insensitive to salt concentration. The weak  $n$ -dependence lends some credit to recent predictions of a model where  $Q$  was assumed to be state-independent [11].

The Helmholtz free energy may be calculated from the density profiles within the mean-field expression consistent with PB theory:

$$F = U - TS, \tag{20}$$

where  $U$  is the electrostatic energy:

$$U = \frac{1}{2} \int_v [\rho_d(\mathbf{r}) + e\rho_c(\mathbf{r})]\varphi(\mathbf{r}) d^3r = U_c + U_d, \tag{21}$$

while the entropy reduces to its ideal part

$$S = -k_B \sum_{\alpha=+,-} \int_v \rho^\alpha(\mathbf{r}) \{ \ln[A^3 \rho^\alpha(\mathbf{r})] - 1 \} d^3r. \tag{22}$$

Use of the PB equation allows  $F$  to be cast in the form

$$F = U_d - U_c + k_B T \{ N_+ [\ln(A^3 \rho_0^+) - 1] + N_- [\ln(A^3 \rho_0^-) - 1] \}. \tag{23}$$

## Spherical Geometry Quadrupolar b.c.

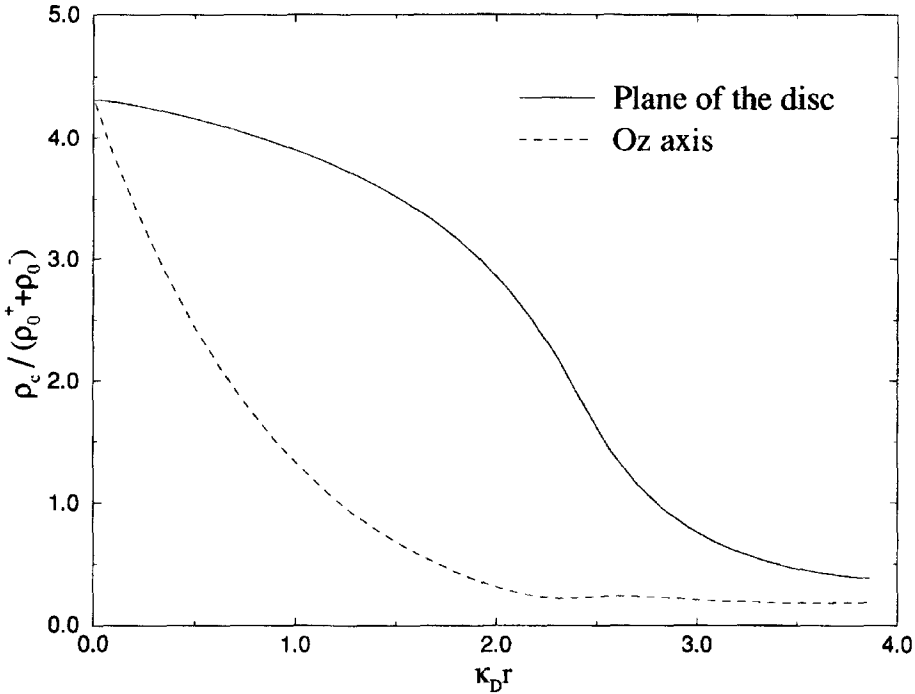


Fig. 1. Charge density profiles  $\rho_c/(\rho_0^+ + \rho_0^-)$  as a function of  $\kappa_D|\mathbf{r}|$ , for a salinity  $n_s = 10^{-3}$  M and  $n = 5.10^{-5}$  M ( $R = 200$  Å,  $\kappa_D R = 3.88$ ). The WS cell is a sphere and the b.c. impose a quadrupolar potential on the sphere. The upper and lower curves represent the profile in the plane of the disc ( $\theta = \frac{1}{2}\pi$ ) and along the  $Oz$ -axis ( $\theta = 0$ ), respectively. The summation in Eq. (9) has been restricted to  $l = 12$ .

The usual isothermal charging procedure [12,6], whereby the surface charge of the disc is varied from 0 to its final value  $q$  while  $N_+$  is kept constant, allows the free energy to be reexpressed as

$$F - F(q = 0) = k_B T \int_0^q dq' \int_{S_d} \ln[A^3 \rho_{q'}^-(\mathbf{r})] d^2r, \tag{24}$$

where  $S_d = \pi r_0^2$  is the area of the disc. On the other hand, if  $N_-$  is constant during the charging process, the resulting expression for  $F$  involves the surface integral of  $-\ln[A^3 \rho_{q'}^+]$ . Expression (24) is valid whenever the normal component of the electric field vanishes on the surface  $S$  of the WS cell; an additional surface term appears when this is not the case. Eq. (24) generalizes the well-known result from Gouy–Chapman theory for a uniformly charged infinite plane [12]. Note that the expression for the free energy is valid within non-linear PB theory, but for explicit calculation, we have used the density profile  $\rho^-(\mathbf{r})$  resulting from the linearized version of the theory. In



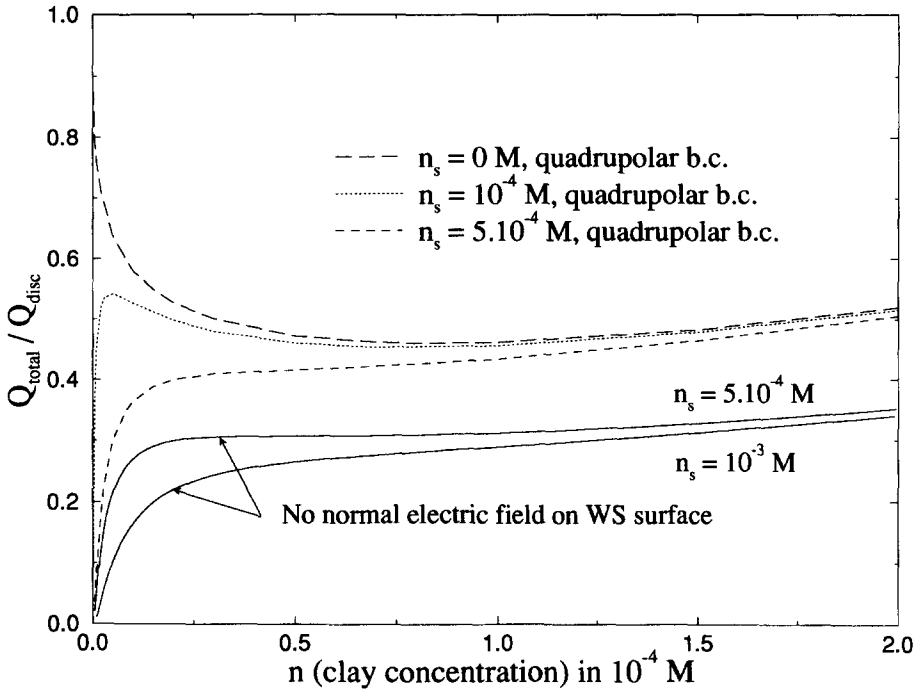


Fig. 2. Variations of the total normalized quadrupole moment  $Q/Q_{disc}$  with clay and salt concentration, for a spherical WS cell. The two lower curves (solid lines) correspond to the b.c. where the total electric field has no normal component to the WS sphere. The dashed curves correspond to quadrupolar b.c.

particular, we have evaluated the free energy from Eq. (24) for a cylindrical WS cell, as a function of the aspect ratio  $h/r_0$  for a fixed volume  $2\pi R^2 h$  and for the two different charging processes ( $N_+$  or  $N_-$  constant) which are strictly equivalent only provided that linearization is justified. Examples are shown in Fig. 3 (large values of  $h/r_0$  can be associated with a tendency towards swelling). We then obtain the density profiles corresponding to the “optimum” WS cylinder shown in Fig. 4. The equilibrium value of  $h/r_0$  is such that  $R/r_0 > 1$ . Swelling is thus restricted under the action of electrostatic forces alone.

Finally, Eq. (4) allows a rapid derivation of a lower bound to the Donnan effect. Indeed

$$\rho_0^+ \rho_0^- = \frac{n_+ n_-}{\left[ \frac{1}{v} \int_v \exp(-\beta e \varphi) d^3 r \right] \left[ \frac{1}{v} \int_v \exp(\beta e \varphi) d^3 r \right]} \tag{25}$$

By virtue of the Schwartz inequality

$$\left[ \frac{1}{v} \int_v \exp(-\beta e \varphi) d^3 r \right] \left[ \frac{1}{v} \int_v \exp(\beta e \varphi) d^3 r \right] \geq 1, \tag{26}$$

## Aspect ratio dependence of the free energy

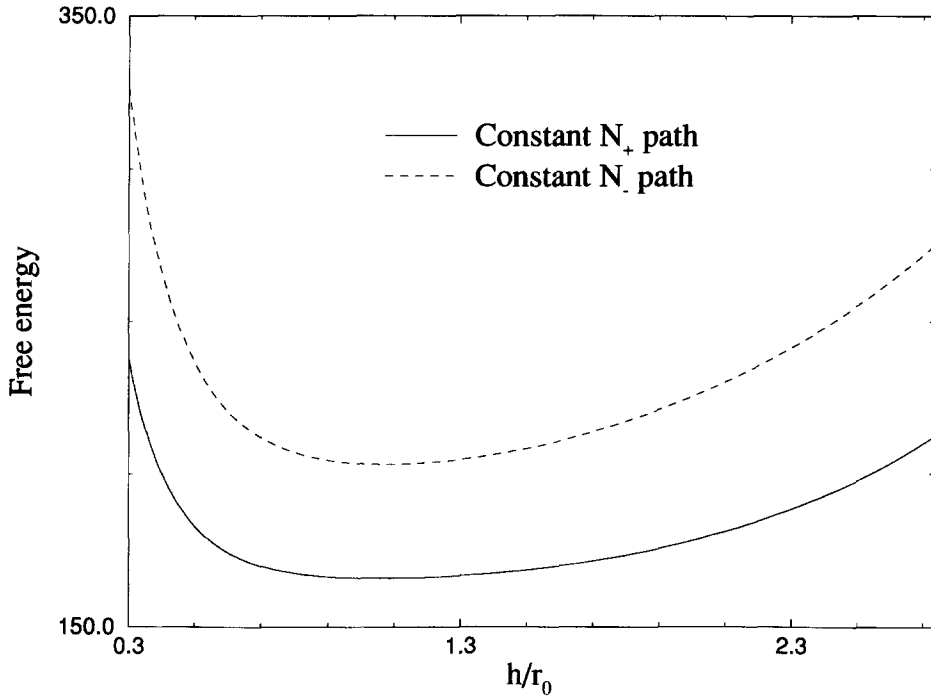


Fig. 3. Determination of the “optimum” cylindrical cell for  $n_s = 10^{-3}$  M and  $n = 5 \cdot 10^{-5}$  M. The only aspect-ratio-dependent contribution to the free energy  $F$  is  $\int_0^q dq' \int_{disc} \phi_{q'}(r, z = 0) d^2r$ , which has been plotted versus  $h/r_0$ , the volume  $2\pi R^2 h$  being kept constant. The two curves correspond to charging processes where either coion or counterion concentrations are kept constant. They both give the same minimum  $h/r_0 \simeq 1.03$  (i.e.  $R/r_0 \simeq 1.62$ ,  $R/h \simeq 1.57$ ). The summation in Eq. (13) has been restricted to  $n = 200$ .

it may be concluded that

$$\rho_0^+ \rho_0^- \leq n_+ n_- = n_s^2 \left[ 1 + \frac{Z}{V n_s} \right]. \quad (27)$$

If the suspension is in osmotic equilibrium with a salt solution of concentration  $n'_s$ , then the condition of chemical equilibrium between the salt ions in the suspension and in the solution implies that [4]  $\rho_0^+ \rho_0^- = (n'_s)^2$ . Substitution into (27) leads to the required inequality:

$$\frac{n_s}{n'_s} \geq \sqrt{1 + \frac{Z^2}{4V^2 n_s'^2}} - \frac{Z}{2V n'_s}. \quad (28)$$

In the Debye–Hückel (linearized PB) limit, the inequality becomes an equality, thus providing an estimate of the Donnan effect.

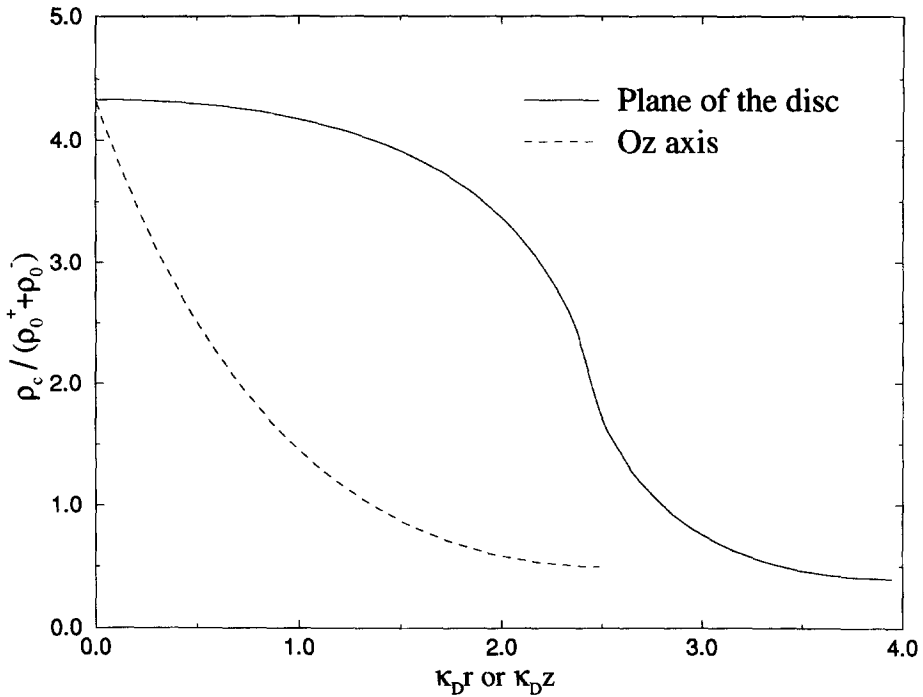


Fig. 4. Charge density profiles versus  $\kappa_D r$  (upper curve, corresponding to  $z = 0$ ), or versus  $\kappa_D z$  (lower curve, corresponding to  $r = 0$ ), for a WS cylinder. The concentrations are the same as in Fig. 3,  $h/r_0 = 1.03$  (cf. above), which gives  $\kappa_D r_0 \simeq 2.43$ ,  $\kappa_D h \simeq 2.50$  and  $\kappa_D R \simeq 3.94$ .

## 5. Conclusion

Our linearized PB analysis provides explicit expressions for the density profiles of co- and counterions in the electric double layer around a single, uniformly charged disc confined to a spherical or cylindrical Wigner–Seitz cell. This approach accounts for the finite concentration of such model clay platelets. Linearization of the Boltzmann factor is, strictly speaking, only justified provided the variations of the potential throughout the cell are small compared to  $k_B T/e$ . The condition is fulfilled if the Gouy length exceeds the Debye screening length  $\lambda_D$ , which requires a low surface charge and/or a high concentration of added salt. However, even outside the strict range of validity, the linearized theory may be expected to provide a qualitative picture of the electric double layer around a platelet of finite size.

A key result of the present analysis is the rather weak dependence of the quadrupole moment of the double layer on clay and salt concentration, except at very low concentration of polyanions.

The linearized PB analysis may be improved, in the immediate vicinity of the disc, by incorporating in some adequate manner the known analytic or semi-analytic solutions of the one-dimensional PB equation for an infinite uniformly charged plane in a WS slab.

We are presently examining in more detail the results of our analysis for the osmotic pressure and swelling. A comparison will be made with numerical solutions of the PB equation in a cubic WS cell with periodic boundary conditions [13] in the perspective of density-functional Monte Carlo simulations similar to those which have proved successful for spherical charge-stabilized colloids [5].

### **Acknowledgements**

The authors benefited from stimulating conversations with Jean-Louis Barrat, Alfred Delville, Marjolein Dijkstra, Pierre Levitz and Paul Madden. JPH gratefully acknowledges the hospitality of the Physical and Theoretical Chemistry Laboratory, and Balliol College, Oxford.

### **References**

- [1] H. van Olphen, *Clay Colloid Chemistry*, 2nd Ed. (Wiley, New York, 1977).
- [2] G. Gouy, *J. Phys.* 9 (1910) 457; D.L. Chapman, *Phil. Mag.* 25 (1913) 475.
- [3] A. Delville and P. Laszlo, *Langmuir* 6 (1990) 1289.
- [4] M. Dubois, T. Zemb, L. Belloni, A. Delville, P. Levitz and R. Setton, *J. Chem. Phys.* 98 (1992) 2278.
- [5] H. Löwen, J.P. Hansen and P.A. Madden, *J. Chem. Phys.* 98 (1993) 3275.
- [6] One of the first examples of Poisson–Boltzmann calculations for polyelectrolytes in a Wigner–Seitz cell is the work by R.A. Marcus, *J. Chem. Phys.* 23 (1955) 1057.
- [7] Laporte Inorganics Laponite Technical Bulletin L104/90/A.
- [8] R.B. Secor and C.J. Radke, *J. Colloid Interface Sci.* 103 (1985) 237; F.R.C. Chang and G. Sposito, *J. Colloid Interface Sci.* 163 (1994) 19.
- [9] G.N. Watson, *A Treatise on the Theory of Bessel Functions*, 2nd Ed. (Cambridge University Press, Cambridge, 1958).
- [10] Ch. Gruber, J.L. Lebowitz and Ph.A. Martin, *J. Chem. Phys.* 75 (1981) 944.
- [11] M. Dijkstra, J.P. Hansen and P.A. Madden, *Phys. Rev. Lett.* 75 (1995) 2236.
- [12] E.J.W. Verwey and J.Th.G. Overbeek, *Theory of the Stability of Lyophobic Colloids* (Elsevier, New York, 1948).
- [13] M. Dijkstra, E. Trizac, J.P. Hansen and P.A. Madden, to be published.